PHYSICAL REVIEW B **77**, 161404(R) (2008)

Measurement and density functional calculations of optical constants of Ag and Au from infrared to vacuum ultraviolet wavelengths

Wolfgang S. M. Werner*
Institut für Allgemeine Physik, Vienna University of Technology, Wiedner Hauptstraße 8-10, A 1040 Vienna, Austria

Michael R. Went and Maarten Vos
Atomic and Molecular Physics Laboratories, Research School of Physical Sciences and Engineering, Australian National University, Canberra ACT 0200, Australia

Kathrin Glantschnig
Institut für Physik, Fachbereich Theoretische Physik, University of Graz, Universitätsplatz 5, A 8010 Graz, Austria and University of Leoben, Franz-Josefstraße 18, A 8700, Austria

Claudia Ambrosch-Draxl
Lehrstuhl für Atomistic Modelling and Design of Materials, University of Leoben, Franz-Josefstraße 18, A 8700, Austria
(Received 17 January 2008; published 15 April 2008)

The dielectric function of Ag and Au for wavelengths ranging from the infrared to the vacuum ultraviolet regime was measured with reflection electron energy-loss spectroscopy (REELS). The spectra are compared to density functional theory (DFT) calculations and to experimental optical data available in the literature since about three decades ago. The REELS and DFT results exhibit good consistency, while the earlier optical data significantly deviate. The results demonstrate that REELS and DFT are powerful tools for the study of the electromagnetic response of surfaces.

DOI: 10.1103/PhysRevB.77.161404 PACS number(s): 79.20.Fv, 71.20.Mq, 79.20.Kz, 61.43.Dq

Optical constants of a solid are not only of fundamental relevance in many branches of science but also have many practical applications. In spite of their importance, no comprehensive database exists for optical spectra of arbitrary materials at all frequencies. A fundamental understanding of the underlying physics requires a theoretical background, which has not been widely explored until the last decade from an *ab initio* point of view. Nowadays, it has become more common to perform first-principles calculations of the frequency-dependent dielectric function of arbitrary solids[1,2] within the framework of density functional theory (DFT) and beyond.

Experimental data against which these theories can be tested have been compiled by Palik[3] and usually consist of a number of individual data sets taken over different wavelength ranges. The main difficulty with optical measurements over a wide energy scale is related to the vanishing rest mass of the photon which, by virtue of energy and momentum conservation, implies that the overwhelming majority of scattering processes lead to absorption of the probing particle. Therefore, the spectrum is divided into regions of high opacity and high transparency for which accurate simultaneous determinations of the dispersive (real) and absorptive (imaginary) parts of the dielectric function are more involved. Often, complementary data from other sources are used and a Kramers-Kronig analysis is invoked.[4] For these reasons, the use of electron energy-loss measurements as a probe of the dielectric response of a solid represents an attractive alternative that provides information on the entire range between the infrared and x-ray wavelengths. However, the finite electron rest mass makes it *highly unlikely* for an electron to be absorbed during scattering leading to strong multiple scattering features in the loss spectra. Therefore, it is necessary to deconvolute the spectra before optical data can be derived from them. Such measurements have been routinely carried out in the transmission electron microscope in the past,[5] but this technique is quite involved when it comes to sample preparation. Moreover, the measurements are only rarely carried out in ultrahigh vacuum. A method that is free of these deficiencies is the reflection electron energy-loss spectroscopy (REELS), but the data analysis is more complicated and an appropriate approach has only been reported recently[6] and has been tested for several solids,[6–8] including Ag and Au, which are studied in the present work.

However, in these works, the full width at half maximum (FWHM) of the elastic peak amounted to about 1.7 eV, implying that the intensity of the elastic peak is significantly higher than or comparable to the intensity of the loss features for energy losses of up to ~4 eV, which makes elimination of the elastic peak less reliable in this energy range. Therefore, important features in the loss function and the dielectric function in the visible and near visible range could not be retrieved with good accuracy. In particular, the surface plasmon feature in the Ag spectrum at ~3.8 eV, which is highly relevant for the field of plasmonics,[9] is obscured in this way by the dynamic range of the REELS data. In the present Rapid Communication, high-resolution electron energy-loss spectra measured in reflection[10] are analyzed to give the optical spectra of Ag and Au between the infrared and vacuum ultraviolet (VUV) range of wavelengths. An evaluation with respect to DFT calculations reveals that the present approach leads to more reliable dielectric functions compared to existing earlier optical data.

The dielectric response is calculated within the random phase approximation, where the excited electron and the cre-

ated hole are regarded to be independent (independent particle approximation),

$$\mathrm{Im}\,\epsilon(\omega) = \frac{\hbar^2 e^2}{\pi m^2 \omega^2} \sum_{n,n'} \int_{\mathbf{k}} p_{n',n,\mathbf{k}} p_{n',n,\mathbf{k}} \times [f(\varepsilon_{n,\mathbf{k}}) - f(\varepsilon_{n',\mathbf{k}})] \delta(\varepsilon_{n',\mathbf{k}} - \varepsilon_{n,\mathbf{k}} - \omega) d\mathbf{k}, \quad (1)$$

with $p_{n',n,\mathbf{k}}$ representing the momentum matrix element between bands n and n' for a $\mathbf{k}$ point in the irreducible part of the Brillouin zone and $f(\varepsilon_{n,\mathbf{k}})$ being the occupation number of the corresponding single-particle state with energy $\varepsilon_{n,\mathbf{k}}$. A lifetime broadening of 0.1 eV for the interband transitions is used, while for the intraband contribution ($n=n'$), a Drude-type line shape is adopted with broadenings of 0.1 eV for Au and 0.02 eV for Ag (corresponding to a lifetime τ of 31×10^{-15} s as given in Ref. 11). The real part of the dielectric function is obtained by a Kramers-Kronig transformation.

This approach is well suited for metals where the Coulomb interaction of the electron-hole pair is efficiently screened. The quasiparticle energies and wave functions are approximated by the Kohn-Sham eigenstates, which are obtained by the linearized augmented plane wave (LAPW) method using the WIEN2K code.[12] Exchange and correlation effects are treated by the generalized gradient approximation parametrized by Perdew *et al.*[13] Spin-orbit interaction is included via a second variational scheme. The theoretical framework to compute the dielectric function within the LAPW scheme is described in Ref. 2. Well converged spectra are calculated on a $51 \times 51 \times 51$ $\mathbf{k}$-point grid consisting of 3276 irreducible points, with the Brillouin zone integrations carried out by the linear tetrahedron method.

REELS spectra analyzed in the present work were obtained on polycrystalline Ag and Au samples using the high-energy electron scattering spectrometer at the Australian National University operating at a base pressure of 1×10^{-10} mbar.[16] Sample cleaning was performed by Xe^+ ion bombardment. The incidence and emission angles were 45° with respect to the surface normal, the scattering angle was 120°, and the analyzer (half polar) opening angle was about 0.5°. The energy resolution varied with energy but was always better than 0.5 eV (FWHM of the elastic peak). The spectra for primary energies of 5 and 40 keV are shown in Fig. 1.

When an electron hits a solid surface, it experiences multiple elastic and inelastic collisions. The boundary conditions of Maxwell's equations lead to volume excitations experienced deep inside the solid as well as surface excitations occurring both in vacuum and inside the solid upon crossing the solid-vacuum interface. The loss spectrum is a superposition of groups of electrons that have experienced multiple surface and volume energy losses. Therefore, the employed deconvolution procedure[8,14] for elimination of multiple scatterings giving the single-scattering loss distribution in an individual volume excitation $w_b(T)$ and surface excitation $w_s(T)$ requires a simultaneous analysis of *two* loss spectra for which the relative importance of surface and volume excitations is different.

The probability for experiencing a surface excitation de-

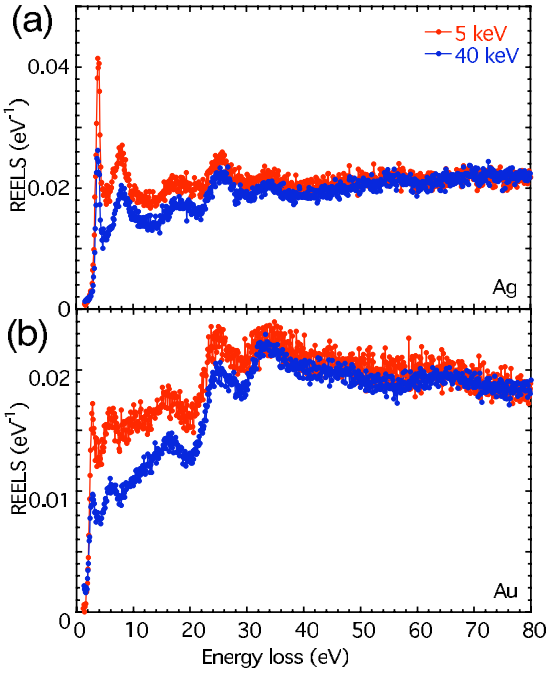

FIG. 1. (Color online) Experimental REELS for electron energies of 5 (light symbols) and 40 (dark symbols) keV. (a) Ag; (b) Au.

creases with increasing energy. Therefore, the procedure mentioned above can be applied to two spectra taken at sufficiently different energies. In Fig. 1, the decrease in the surface excitation probability is clearly evidenced by the decrease in intensity for energies below 30 eV when the primary energy is increased from 5 to 40 keV. The resulting single-scattering loss distributions are shown in Fig. 2 as data points. These single-scattering distributions are in good agreement with results of the earlier analysis for energies above ~5 eV [not shown (see Ref. 7)]. The insets of Fig. 2 demonstrate that with the energy resolution of the present measurements, the peak at 3.8 eV in the Ag spectra can be decomposed into a contribution of a surface excitation at 3.7 eV and a volume excitation at 3.9 eV, while a clear assignment is not possible on the basis of the earlier measurements. The differences between these deconvoluted spectra and the raw data in Fig. 1, in particular, above 50 eV, clearly show the influence of multiple scatterings on REELS.

In the next step of the analysis, the single-scattering loss distributions are fitted to theory[14] using an appropriate model dielectric function consisting of a set of the Drude-Lindhard oscillators,[17]

$$\varepsilon_1(\omega,q) = 1 - \sum_i \frac{f_i[\omega^2 - \omega_i(q)^2]}{[\omega^2 - \omega_i(q)^2]^2 + \omega^2\gamma_i^2},$$

$$\varepsilon_2(\omega,q) = \sum_i \frac{f_i\gamma_i\omega}{[\omega^2 - \omega_i(q)^2]^2 + \omega^2\gamma_i^2}, \quad (2)$$

where $\omega=T$ is the energy loss and q is the momentum transfer. Here, f_i represents the oscillator strength, γ_i is the damping coefficient, and ω_i is the energy of the ith oscillator. A quadratic dispersion $\omega_i(q)=\omega_i+q^2/2$ is assumed. Those val-

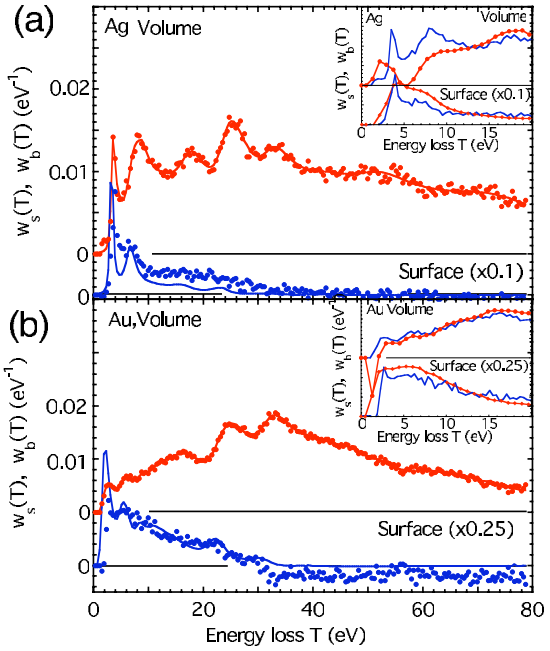

FIG. 2. (Color online) Retrieved surface and volume single-scattering loss distributions (data points) and fit to the theory summarized in Ref. 14 using the model dielectric function given by Eq. (2) (solid curves). (a) Ag; (b) Au. The insets compare the low-energy part of the present analysis (solid curves) with earlier data (Ref. 7) (solid curves with data points).

ues of the Drude-Lorentz parameters in the above equation, which minimize the deviation between experiment and theory,[14] are taken to parametrize the dielectric function. Since various aspects of the surface scattering process, such as its depth and angular dependence, cannot be modeled by means of the simple formulas in Ref. 14 with the same level of accuracy as the volume scattering process, the latter was given a relative weight factor of 100 in the fitting procedure. The solid curves in Fig. 2 represent the result of this approach for the present data set.

In Fig. 3, the loss function ($\mathrm{Im}\{-1/\varepsilon(0,\omega)\}$) as well as the real $[\varepsilon_1(0,\omega)]$ and imaginary $[\varepsilon_2(0,\omega)]$ parts of the dielectric functions of Ag and Au calculated within the DFT framework (solid curves) and derived from REELS (circles) are compared to the data from Palik's book[15] (dashed curves). The fitting procedure yields the loss functions $\mathrm{Im}\{-1/\varepsilon(0,\omega)\}$, as shown in the left panels of Fig. 3. Integrating these over the region of allowed momentum transfers gives the single-scattering loss distributions in the upper panels in Fig. 2. Since the model dielectric function [Eq. (2)] satisfies the Kramers-Kronig dispersion relationships, the real and imaginary parts of the dielectric function can also be directly evaluated from the fit parameters describing the loss function. These quantities are shown in the middle and right-hand-side panels of Fig. 3. However, the measurements mainly sample the absorptive part of the spectrum. Therefore, by assuming that the experimental error in $\mathrm{Im}\{-1/\varepsilon\}$ is of the order of 5%–10%, the error bars for ε_1 and ε_2 can be estimated using the common rules of error propagation. This leads to experimental errors in ε_1 and ε_2 of the same order of magnitude for energies above 10 eV, but for smaller energies they can become excessively large and may exceed 100%, as indicated in the figure by the error bars at selected energies. In Ref. 18, the error introduced by the deconvolution procedure has been estimated to be well below 10%.

The DFT results display a wealth of fine structure in the dielectric function. Taking into account the finite energy resolution of the REELS measurements of about 0.5 eV as well as the fact that the single-scattering loss distributions represent an average over all allowed momentum transfers, the consistency between the REELS and DFT results is satisfactory, while the agreement with Palik's data is less good. In particular, peaks in the REELS and DFT results for ε_1, ε_2 and $\mathrm{Im}\{-1/\varepsilon\}$ in the range between 20 and 40 eV are slightly shifted in position, with respect to the earlier optical spectra. The peaks in the range between 40 and 50 eV, which are the strongest ones in the DFT results for $\mathrm{Im}\{-1/\varepsilon\}$, are less intense in the REELS data. This fact can be traced back to local-field effects (LFEs) that are not accounted for in the present calculations. As found for TiO_2,[19] the LFEs shift the spectra in this energy range to higher energies, thereby sig-

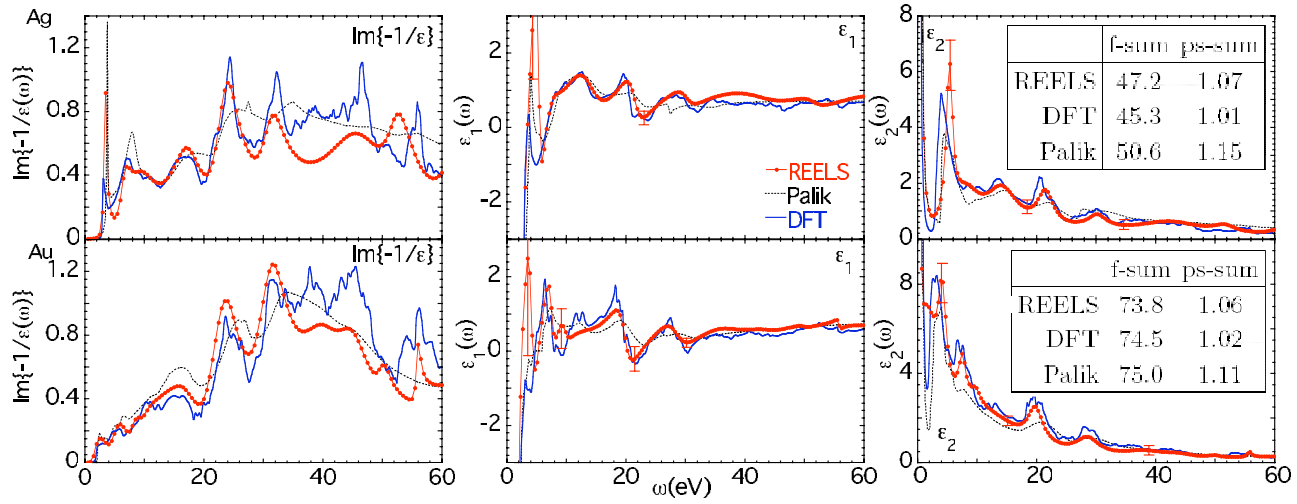

FIG. 3. (Color online) Loss function $\mathrm{Im}\{-1/\varepsilon\}$ as well as dispersive ε_1 and absorptive part ε_2 of the dielectric function of Ag and Au retrieved from the REELS spectra (circles) compared to Palik's data (Ref. 15) (dashed curves) and to DFT results (solid curves).

nificantly reducing the magnitude. The only pronounced feature where the REELS results agree significantly better with Palik's data for the loss function [Fig. 3(a)] is the peak at about 4 eV for Ag. In this energy range, there are uncertainties stemming from the DFT *d* band positions which are deviating from experiment by some tenths of an eV. At the same time, further clarification is needed concerning the role of surface effects in the density functional calculations. This is particularly important in view of the growing field of plasmonics.

Sum rule checks are summarized in the insets of Fig. 3. The REELS and DFT data above 60 eV were extended to 30 keV by the empirical x-ray scattering data of Henke *et al.*[20] For the Thomas-Reiche-Kuhn sum rule (or *f*-sum rule), with an expectation value equal to the atomic number, all three data sets show deviations of the same order of magnitude. In the present context, the perfect screening (*ps*) sum rule, with an expectation value of unity, seems to be more important since it emphasizes low energies of <100 eV. The *ps*-sum rule is accurately satisfied by the DFT calculations, while the REELS data and Palik's data exhibit deviations of up to 7% and 15%, respectively.

Two powerful methods to obtain optical data, DFT calculations and REELS, have been compared over a large wavelength range between the infrared and the VUV for Ag and Au. Within the experimental error, satisfactory agreement was found between experiment and theory, while the optical data measured several decades ago[3] significantly deviate. Since REELS is conceivably one of the simplest experiments with electrons, it is expected to become a useful tool for investigating the dielectric response of a solid and theoretical modeling of associated phenomena.

The support by the Australian Research Council and the Austrian Science Foundation FWF (Projects No. P15938-N02 and No. P16227-N08) is gratefully acknowledged.

*werner@iap.tuwien.ac.at

[1] G. Onida, L. Reining, and A. Rubio, Rev. Mod. Phys. **74**, 601 (2002).
[2] C. Ambrosch-Draxl and J. O. Sofo, Comput. Phys. Commun. **175**, 1 (2006).
[3] E. D. Palik, *Handbook of Optical Constants of Solids I & II* (Academic Press, Orlando, Florida 1985).
[4] D. Y. Smith, *Handbook of Optical Constants of Solids I & II* (Academic Press, Orlando, Florida 1985), Chap. 3, Vol. I.
[5] R. F. Egerton, *Electron Energy Loss Spectroscopy in the Electron Microscope* (Plenum, New York, 1985).
[6] W. S. M. Werner, Surf. Sci. **600**, L250 (2006).
[7] W. S. M. Werner, Appl. Phys. Lett. **89**, 213106 (2006).
[8] W. S. M. Werner, Surf. Sci. **601**, 2125 (2007).
[9] T. W. Ebbesen, H. J. Lezec, H. F. Ghaemi, T. Thio, and P. A. Wolff, Nature (London) **391**, 667 (1998).
[10] W. S. M. Werner, M. R. Went, and M. Vos, Surf. Sci. **601**, L109 (2007).
[11] P. B. Johnson and R. W. Christy, Phys. Rev. B **6**, 4370 (1972).
[12] P. Blaha, K. Schwarz, G. K. H. Madsen, D. Kvasnica, and J. Luitz, *WIEN2k, an augmented plane wave and local orbitals program for calculating crystal properties* (Vienna University of Technology, Vienna 2001).
[13] J. P. Perdew, K. Burke, and M. Ernzerhof, Phys. Rev. Lett. **77**, 3865 (1996).
[14] W. S. M. Werner, Phys. Rev. B **74**, 075421 (2006).
[15] E. D. Palik, *Handbook of Optical Constants of Solids* (Academic, New York, 1985).
[16] M. R. Went and M. Vos, Appl. Phys. Lett. **90**, 072104 (2007).
[17] Y. F. Chen, C. M. Kwei, and C. J. Tung, Phys. Rev. B **48**, 4373 (1993).
[18] M. R. Went, M. Vos, and W. S. M. Werner, Surf. Sci. (to be published 2008).
[19] N. Vast, L. Reining, V. Olevano, P. Schattschneider, and B. Jouffrey, Phys. Rev. Lett. **88**, 037601 (2002).
[20] B. L. Henke, E. M. Gullikson, and J. C. Davis, At. Data Nucl. Data Tables **54**, 181 (1993).